Ornamental Plant Research

ARTICLE

Open Access

https://doi.org/10.48130/opr-0025-0033
Ornamental Plant Research **2025**, 5: e037

Developing a homology-driven gene silencing system in *Iris japonica*: a versatile tool for comparative functional studies

Cheng Luo[1], Zhiyan Wu[1], Lingmei Shao[1], Jiaping Zhang[1], Yiping Xia[1*] and Danqing Li[2*]

[1] *Genomics and Genetic Engineering Laboratory of Ornamental Plants, Department of Horticulture, College of Agriculture and Biotechnology, Zhejiang University, Hangzhou 310058, China*
[2] *Department of Landscape Architecture, School of Civil Engineering and Architecture, Zhejiang Sci-Tech University, Hangzhou 310018, China*
* Corresponding authors, E-mail: ypxia@zju.edu.cn; danqingli@zju.edu.cn

Abstract

Iris japonica, an evergreen ornamental species known for its beautiful flowers and year-round evergreen foliage, is difficult to genetically manipulate due to the lack of an efficient genetic transformation system. This limitation hinders the functional verification of key genes in *I. japonica*. To address this, a Virus-Induced Gene Silencing (VIGS) system based on Tobacco rattle virus (TRV) was developed, enabling efficient, transient gene silencing in *I. japonica*. In this system, the *phytoene desaturase* (*PDS*) gene, a common reporter gene used for VIGS, was selected to assess the silencing efficiency. The recombinant vector pTRV2-*IjPDS* was used to infect *I. japonica* plants. The *PDS* gene silencing resulted in distinct photobleaching symptoms, demonstrating the successful silencing of the target gene. The presence of the TRV vector was verified by using a GFP-tagged pTRV2-GFP vector, and GFP expression was detected using fluorescence visualization under ultraviolet (UV) light and confirmed by laser confocal microscopy. Real-time PCR was used to quantify the reduction in *IjPDS* gene expression, confirming the successful silencing. The study further optimized the VIGS system by evaluating the impact of seedling ages on silencing efficiency, identifying one-year-old seedlings as the most effective for gene silencing (36.67%). This TRV-based VIGS system provides a robust tool for functional gene analysis in *I. japonica* and offers a new approach to studying the rules of key genes in its biological processes, with potential applications in ornamental plant breeding and genomics research.

Citation: Luo C, Wu Z, Shao L, Zhang J, Xia Y, et al. 2025. Developing a homology-driven gene silencing system in *Iris japonica*: a versatile tool for comparative functional studies. *Ornamental Plant Research* 5: e037 https://doi.org/10.48130/opr-0025-0033

Introduction

Iris species (Iridaceae) are one of the most horticulturally important perennial herbaceous plants, renowned for their ornamental value, widely used in garden landscaping and floral design[1–3]. Among them, *Iris japonica* is highly prized for its elegant flowers and year-round evergreen foliage[4–6]. In addition to its aesthetic appeal, *I. japonica* also holds medicinal significance, containing various bioactive compounds used in traditional herbal remedies and contemporary health products[7,8]. *I. japonica* is not only a horticultural species, but also a source of bioactive compounds with antioxidant and medicinal properties[9,10]. However, compared to other *Iris* groups with a rich diversity of horticultural cultivars, such as Louisiana irises and Japanese irises, *I. japonica* has fewer horticultural cultivars and limited variation in key traits, which affects its resource development and utilization.

The primary obstacle to advancing the genetic improvement of *I. japonica* lies in the lack of a reliable and efficient genetic transformation system. This limitation hinders the functional validation of key genes that could enhance desirable traits, such as stress tolerance, flower quality, and medicinal properties. In recent years, transient transformation methods have emerged as a promising approach to bypass the need for stable transformation systems, allowing for rapid gene silencing and functional analysis in non-model plants. In the diverse order of orchids, virus-induced gene silencing (VIGS) has been used to dissect the functions of genes regulating flower morphogenesis and flowering time[11–13]. In apple, VIGS has been implemented using the Apple Latent Spherical Virus (ALSV) as a vector, facilitating the study of genes associated with fruit development and quality[14]. Similarly, researchers have utilized the *phytoene desaturase* (*PDS*) gene as a reporter to evaluate the efficacy of VIGS systems in tea plants[15].

VIGS is a widely utilized transient transfection technique that employs viruses carrying cDNA fragments of target genes to infect plants[16]. It leverages a plant's natural response to viral infections to suppress the expression of specific target genes[17]. Unlike stable genetic transformation, VIGS does not require the generation of stable transgenic lines, making it particularly valuable for species that are difficult to transform. This RNA silencing method operates by using viral vectors to deliver fragments of the target gene into plant cells, where they activate the plant's RNA interference (RNAi) machinery. This results in the degradation of the corresponding mRNA and a subsequent reduction in the expression of the target gene. Recently, several viral vectors have been modified for VIGS to bring a larger collection of monocots under the ambit of this method[18], including Tobacco Mosaic Virus (TMV), Tobacco Rattle Virus (TRV)[19], Foxtail Mosaic Virus (FMS)[20], and Barley Stripe Mosaic Virus (BSMV)[21]. Among these, the TRV vector has gained popularity due to its lighter symptoms of plant viruses, longer duration and higher silencing efficiency, resulting in the induction of gene silencing in a broad range of plant species. It has been successfully applied to both dicots and monocots such as wheat (*Triticum aestivum*) and maize (*Zea mays*)[22,23].

VIGS has already been successfully applied to a range of ornamental plants, including species like gerbera (*Gerbera hybrida*), rose (*Rosa hybrida*), and lily (*Lilium* spp.). For instance, in gerbera, VIGS has provided insights into the regulation of flower development and secondary metabolism[24], while in roses, it has helped unravel mechanisms controlling petal size and senescence[25,26]. Similarly, in lilies, VIGS has proven useful in identifying key genes involved

in bulb development and growth transition[27,28]. These successes illustrate the versatility of VIGS in functional genomics within ornamental plants. However, while the TRV-VIGS system is well-established in dicotyledonous ornamentals (e.g., *Rosa*), its application in monocot species—especially non-graminaceous ones—remains largely underexplored. Previous studies in monocots (e.g., maize) have documented inherent limitations, such as the rapid loss of insert fragments from the VIGS vector, leading to unstable and inconsistent silencing phenotypes[29]. Although the method have been improved[30], these challenges remain unresolved. To date, no successful TRV-VIGS applications have been reported in *Iris*, likely mainly due to the unique challenges posed by their special biology and the low compatibility of the TRV vector with monocots. This research seeks to address this gap by developing a TRV-based VIGS system for *I. japonica*, aiming to establish a valuable tool for gene function analysis and further expand the potential of VIGS in ornamental plant research.

This study demonstrates the successful development of a TRV-based VIGS system for *I. japonica*, providing an efficient method for gene function analysis in this species. First, the *PDS* gene of *I. japonica* was identified, and the VIGS vector, pTRV2-*IjPDS*, was constructed and used to infect *I. japonica* plants. Subsequently, the functionality of the TRV vector was confirmed through fluorescence detection using a GFP-tagged TRV-GFP vector, and gene expression levels were quantified using quantitative real-time PCR (qPCR). Furthermore, phenotypic and molecular validation of *IjPDS* silencing were conducted, and the infection efficiency at different seedling ages was compared in *I. japonica* to determine the optimal receptor age. The establishment of this system not only facilitates the functional validation of key genes in *I. japonica* but also opens new avenues for studying gene regulatory mechanisms in *Iris* species. Overall, it holds significant potential for improving ornamental traits and advancing genetic research in this valuable plant genus.

Materials and methods

Plant materials and growth conditions

Mature plants of *I. japonica* were planted at the Resource Nursery for Flower Bulbs and Herbaceous Perennials, Zhejiang University, Hangzhou, China. In this study, four groups of *I. japonica* with different seedling ages were used as the research objects, namely one month, two months, one year, and two years. Experimental plants used in each group were of uniform size and free of plant diseases and insect pests. These plants were grown in plastic pots containing equal amounts of peat and vermiculite (v:v = 1:1) and kept in a growth chamber with a day/night temperature range of 25/18 °C, 60% relative humidity, and a 16 h light and 8 h darkness per day. After one week, infection experiments were carried out with *Iris* rhizomes and leaf bases.

Total RNA extraction and identification of *I. japonica phytoene desaturase* (*PDS*) gene

The total RNA was extracted from *I. japonica* leaves using the Tiangen Polysaccharide Polyphenol Kit (Cat# RR047A), and the procedures were carried out according to the instructions of the kit. Afterwards, cDNA was synthesized using PrimeScript™ II, 1st Strand cDNA Synthesis Kit (Takara, Cat# 6210A), according to the instructions provided with the kit, and diluted 20 times for further use.

To identify *I. japonica, PDS* gene sequences from *Iris* transcriptome data (PRJNA486414), *PDS* gene sequences from *Arabidopsis thaliana* (*AtPDS*, NC_003075.7), musk lily (*Lilium longiflorum*, *LlPDS*, BAV_93014.1), daffodil (*Narcissus tazetta*, *NtPDS*, AFH_53816.1), wheat (*Triticum aestivum*, *TaPDS*, ACL_36586.1), and gladiolus (*Gladiolus hybrid*, *GhPDS*, AGI_17588.1) were downloaded from National Center for Biotechnology Information website (www.ncbi.nlm.nih.gov) for sequence alignment. Amino acid sequence alignment of homologous sequences from the above plant species was performed by DNAMAN 5.0 software.

To clone the fragment of *IjPDS* for VIGS vector construction, primers were designed according to the conserved regions obtained by the above sequence alignments. The conserved fragment of *IjPDS* was amplified using the forward and reverse primers of *IjPDS*-F and *IjPDS*-R (Table 1). The cDNA obtained by reverse transcription was amplified by PCR using PrimeSTAR® Max DNA Polymerase (Takara, Cat# R045A) to obtain the conserved *IjPDS* fragment. The PCR procedures were as follows: one cycle of 98 °C (1 min); 30 cycles of 98 °C (10 s), 58 °C (5 s), 72 °C (2 min); and one cycle of 72 °C (10 min). Then, the PCR products were tested by 1% (w/v) agarose gel electrophoresis and cloned into the pEASY-Blunt Zero Cloning Vector (TransGen Biotechnology Co., Ltd, Beijing). The conjugate products were transformed into *Escherichia coli* DH5α (Vazyme, C502-02). Then, positive clones were selected for resistance screening on LB plates containing 50 mg/L of kanamycin after dark culture at 37 °C overnight. The presence of *IjPDS* insert was confirmed by PCR with primers M13-F and M13-R (Table 1), and the recombinant plasmid was further confirmed by sequencing.

Construction of the pTRV2-*IjPDS* vector

pTRV1, pTRV2, and pTRV2-GFP vector plasmids used in this study were presented by the Department of Horticulture, China Agricultural University. The above sequencing verified recombinant plasmid of pEASY-Blunt Zero Cloning Vector containing *IjPDS* fragments was extracted, and this plasmid, together with pTRV2 plasmid, were digested with *Xba* I and *Sac* I at 37 °C for 40 min. The 241 bp *IjPDS* fragment and linearized pTRV2 plasmid were ligated using T4 DNA ligase (Takara, Code No. 2011A) at 16 °C for 3 h.

The conjugate product was transformed into *E. coli* DH5α. After dark culture at 37 °C overnight, monoclones were selected and confirmed by PCR using primers spanning the multiple cloning sites of pTRV2-F and pTRV2-R (Table 1). The verified plasmids of positive clones were extracted and transformed into *Agrobacterium* strain GV3101 (Weidi, AC1001S) by the freeze-thaw method. Also, pTRV1 and pTRV2-GFP plasmids were transformed into *Agrobacterium* strain GV3101, respectively. These recombinant *Agrobacterium* clones were selected on LB plates (containing 50 mg/L kanamycin and 50 mg/L rifampicin). After 2 d of dark culture at 28 °C, positive monoclones of the pTRV2 carrying the *IjPDS* fragment and the pTRV2 expressing GFP were selected for PCR detection using primers pTRV2-F and pTRV2-R mentioned above. The positive pTRV1 monoclones were also confirmed by PCR using primers pTRV1-F and pTRV1-R (Table 1).

Agrobacterium infection of *Iris japonica*

To obtain enough *Agrobacterium* infection solution, 100 μL *Agrobacterium* GV3101 containing pTRV1, pTRV2, pTRV2-GFP, and pTRV2-*IjPDS* were respectively added into 5 mL LB medium containing

Table 1. Primers for gene clone and quantitative real-time PCR analysis.

Primer name	Sequence (5'–3')
IjPDS-F	5'-GCTCTAGAATCACTGGGTGGTCAGGTCC-3'
IjPDS-R	5'-CGAGCTCTTCTCAGCTTCCTGTCAAACCA-3'
M13-F	5'-GTAAAACGACGGCCAGT-3'
M13-R	5'-CAGGAAACAGCTATGAC-3'
pTRV2-F	5'-TGGGAGATGATACGCTGTT-3'
pTRV2-R	5'-CCTAAAACTTCAGACACG-3'
pTRV1-F	5'-TTACAGGTTATTTGGGCTAG-3'
pTRV1-R	5'-CCGGGTTCAATTCCTTATC-3'

50 mg/L kanamycin and 50 mg/L rifampicin. The *Agrobacterium* were cultured overnight at 28 °C, 200 rpm for 16 h, and then were transferred into 150 mL LB liquid medium containing 50 mg/L kanamycin and 50 mg/L rifampicin, 10 mM 2-(4-Morpholino)-Ethane Sulfonic Acid (MES), and 20 μM acetosyringone (AS), shaken at 28 °C, 200 rpm for 16 h. When OD_{600} of the *Agrobacterium* solution was about 2.0, the *Agrobacterium* cells were collected by centrifugation at 4,000 rpm and 25 °C for 10 min and were suspended in 150 mL infection buffer containing 10 mM $MgCl_2$, 10 mM MES and 200 μM AS. Afterwards, the infection buffer containing a ratio of 1:1 (v/v) mixture of pTRV1 either with pTRV2 empty vector (pTRV2), pTRV2-GFP (for GFP expression) or pTRV2-*IjPDS* were incubated for 4 h in a dark condition at 25 °C to activate the *Agrobacterium Vir* gene.

The *Iris* leaf was clipped to a height of 10 cm to facilitate subsequent vacuum treatment, and a cross was gently marked on its back with the needle of a 1 mL syringe. The above mixture was then injected into the center of the cross with the 1 mL syringe, with the needle removed. Ten plants were used per replicate in the pTRV2-GFP experiment, with three replicates in total. In the pTRV2-*IjPDS* experiment, each seedling age treatment included three replicates of ten plants each. When rhizomes were used as infection objects, three holes were pierced in the rhizomes or stem tips using the needles of 1 mL syringes before infection for 10 min. The piercing sites were then submerged in the infection solution and subjected to vacuum treatment at –0.9 kg/cm^2 (–0.09 MPa) for 30 min, followed by 20 min air deflation. The treated plants, along with a control group (untreated for short) without injected bacterial solution, were cultured in a dark environment with 60% humidity at 20 °C for 3 d. They were then cultured under conditions of 60% humidity, 14 h of light, 25 °C, 4,000 lx/10 h of darkness, and 18 °C for 28 d to observe any phenotype changes. Meanwhile, to assess the accuracy and effectiveness of the *Agrobacterium* solution and infection method, *Agrobacterium* containing pTRV1 and pTRV2-GFP was mixed in equal proportions and respectively injected into the leaves of tobacco and *I. japonica*. The plants were then observed after being cultured in the dark at 60% humidity and 20 °C for 3 d.

Phenotypic detection of infected plants

After 3 d of dark incubation of infected tobacco, Portable longwave UV lamp (254 nm, 100 W Black Ray model B, 100 AP, UVP, Upland, CA) was used to observe the leaf morphology and fluorescence effect. Meanwhile, laser confocal microscopy (Olympus FV3000, Kyoto, Japan) was used to detect green fluorescent protein in tobacco mesophyllous cells, which allowed preliminary confirmation of successful pTRV2-GFP infection in tobacco.

For *I. japonica*, after 6 d of infection, the UV lamp was used to observe the leaf morphology and fluorescence effect according to the above methods, and a laser confocal microscope was used to detect green fluorescent protein in the injection area of leaves. Secondly, total RNA from the leaves of wild-type *I. japonica* (untreated), pTRV2-treated (pTRV2), pTRV2-GFP-treated (pTRV2-GFP) and pTRV2-*IjPDS*-treated (pTRV2-*IjPDS*) plants was extracted using Tiangen Polysaccharide Polyphenol Kit (Cat#RR047A) for subsequent experiments. Finally, the photobleaching phenotype in leaves of each group was observed, and the time of phenotype changes was recorded. After the plants were cultured in the climate box for 28 d, the total RNA of the new leaves of the control group, pTRV2-treated group, pTRV2-GFP-treated group and pTRV2-*IjPDS*-treated group were extracted for subsequent experiments.

Expression analysis by semi-quantitative PCR and qPCR

Total RNA (1 μg) from each sample above was reverse transcribed into cDNA using the PrimeScript™ II, 1st Strand cDNA Synthesis Kit (Takara, Cat# 6210A). The resulting cDNA was diluted 20-fold with deionized water for subsequent analyses, including semi-quantitative PCR and qRT-PCR. Specifically, semi-quantitative PCR was performed using primers pTRV2-F and pTRV2-R for pTRV2 expression in the above samples to detect the presence of pTRV2-RNA. qPCR was used to detect the relative expression of *IjPDS* in newborn leaves of control group, infected pTRV2 and pTRV2-*IjPDS* plants.

qPCR was performed on a CFX Connect™ Real-Time PCR Detection System (Bio-Rad, Hercules, CA, USA) using TB Green® Premix Ex Taq (TaKaRa, Kyoto, Japan) as the fluorescent dye. The *IjACTIN* served as the internal reference gene for normalizing gene expression levels. Primer v5.0 was applied for the primer design of *IjPDS* and *IjActin*. The reaction mixture was prepared according to the kit instructions. The amplification program included an initial denaturation at 95 °C for 2 min, followed by 39 cycles of 95 °C for 5 s and 55 °C for 30 s. A melting curve analysis was conducted to verify reaction specificity, with the following conditions: 95 °C for 5 s, 65 °C for 5 s, and 95 °C for 5 s. Relative gene expression levels were calculated using the $2^{-\Delta\Delta C_T}$ method with each reaction performed three times.

Data processing and analysis

To accurately evaluate the silencing efficiency of the pTRV2-*IjPDS* in *I. japonica* at different seedling ages, a specific formula was applied: Silencing efficiency = (Total number of photobleached plants/Total number of treated plants) × 100%. By statistically analyzing the number of photobleached and treated plants, the silencing efficiency of genes can be quantitatively determined, allowing for an intuitive evaluation of the TRV virus effect on *Iris* at various seedling ages.

For gene expression analysis, the software SPSS 29.0 was used for variance analysis. The differences in gene expression between groups were assessed through a systematic analysis of variance. Duncan's test was applied to determine the significance of these differences, with a threshold of $p < 0.05$ considered statistically significant. The expression differences of GFP and *IjPDS* in *I. japonica* were analyzed accordingly. Excel 2010 was used to generate bar charts.

Results and discussion

Experimental workflow of virus-induced gene silencing in *Iris japonica*

To achieve virus-induced gene silencing in *I. japonica*, the TRV-based VIGS system was constructed. The workflow for the VIGS system involves several key steps: amplification of the target gene sequence fragment, construction of the recombinant plasmid, selection of recipient plant material, infection with *Agrobacterium tumefaciens,* observation of phenotype, and molecular validation of the silenced gene. Molecular validation includes PCR detection of the inserted target gene and vectors, and gene expression analysis of the target gene in the infected plants (Fig. 1).

For the VIGS vector construction, the TRV virus, which has a bipartite genome, is used. Genome 1 (orange) is integrated into the vector backbone without modification, while Genome 2 (green) carries the coat protein (CP) and is responsible for the silencing activity. The target gene sequence is cloned into Genome 2 to construct the recombinant VIGS vector. The expression of the viral genomes is driven by strong promoters, such as p35S or 2xp35S, ensuring efficient replication and silencing of the target gene.

The *PDS* gene was selected as the target for silencing due to its critical role in carotenoid biosynthesis. Silencing of the *PDS* gene leads to a characteristic photobleached phenotype, with chlorotic or

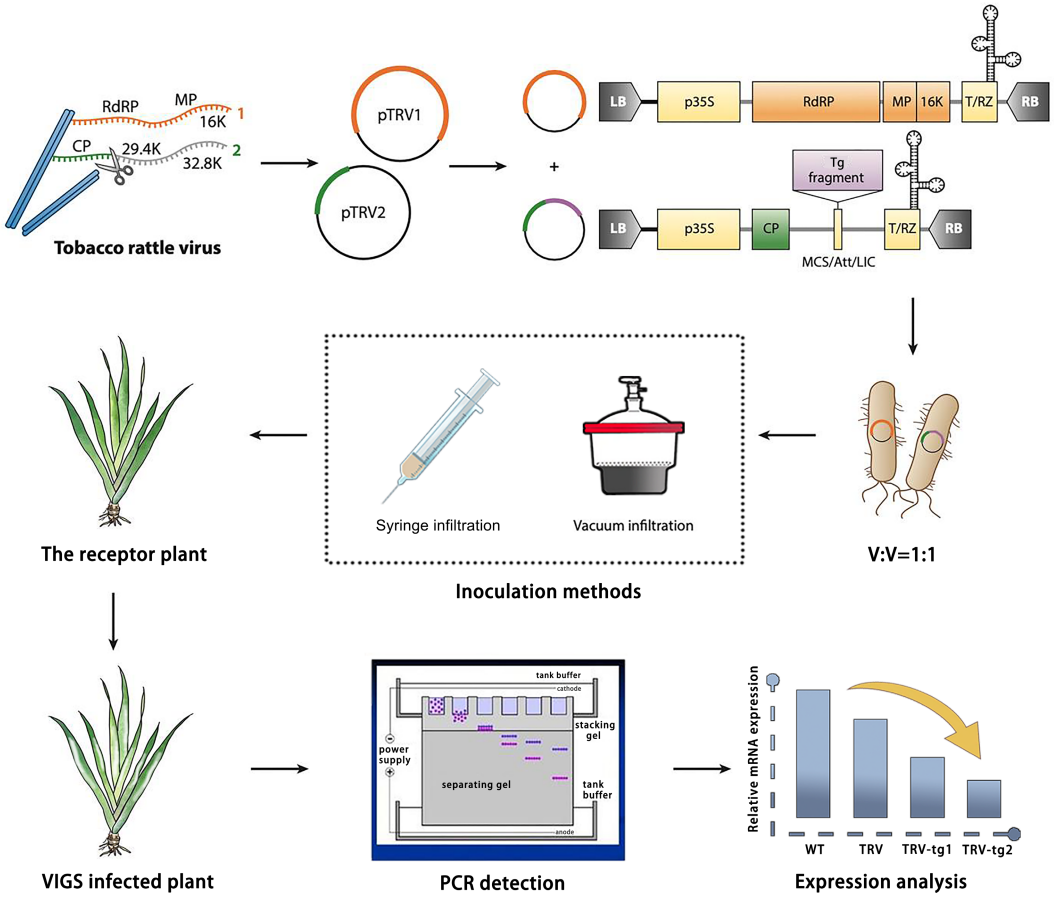

Fig. 1 Design and application of TRV-based virus-induced gene silencing (VIGS) in *Iris japonica*. TRV has a bipartite genome (genome 1 in orange; genome 2 in green). Genome 1 is incorporated into a vector backbone without modification, while only the coat protein (CP) for genome 2 is essential for VIGS. TRV vectors, like the binary pTRV1/pTRV2 system, are typically introduced into plants via *Agrobacterium tumefaciens* inoculation, with T-DNA borders (LB and RB) added. Strong promoters (e.g., p35S or 2×p35S) drive viral genome expression (yellow boxes show required elements for transcription). The vector may also include terminators (e.g., NOS), a self-cleaving ribozyme (T/RZ), and a multiple cloning site (MCS) or recombination system for reliable insertion cloning. For TRV-based VIGS, a target (e.g., *IjPDS*) gene fragment is inserted into the vector, which is then used to infect the receptor material via *A. tumefaciens*. Afterwards, the phenotype is observed, and gene function is validated by the phenotype observation (photobleached leaves), PCR detection, and gene expression analysis.

white patches on the leaves. This makes *PDS* an ideal marker for confirming successful gene silencing. The photobleaching phenotype serves as a visual indicator of effective gene silencing, providing an easily observable marker of the VIGS system's success.

Given the spatial limitations of the viral shell and the potential instability of VIGS, the size of the target gene fragments inserted into the VIGS system is typically restricted to 200–400 bp. These small fragments are sufficient to achieve effective gene silencing while maintaining specificity. The binary TRV vectors, pTRV1 and pTRV2, are then introduced into *I. japonica* via *A. tumefaciens* inoculation. The *Agrobacterium* solutions containing pTRV1 and pTRV2 (with the target gene inserted into pTRV2) are mixed in a 1:1 ratio and inoculated into *I. japonica* plants. Various inoculation methods, such as vacuum infiltration or syringe infiltration, can be used.

After infection, plants are monitored for phenotypic changes, particularly the appearance of the photobleached phenotype, which indicates successful silencing of the *PDS* gene. Control plants are included in each experiment to account for any potential viral instability or off-target effects. Once the phenotypic evidence of silencing is observed, the success of gene silencing is further validated by molecular methods. PCR detection of the inserted fragment and the vectors, along with qPCR analysis of target gene expression levels, were used to quantify silencing efficiency, confirm the knockdown of *IjPDS*, and assess the extent of silencing.

The progress in genetic functional validation and identification research for *Iris japonica* is a slow process. This study is the first to establish a functional TRV-VIGS system in *I. japonica*, a rhizomatous monocot within the Iridaceae family. Unlike the well-studied *Gladiolus hybridus*[31], which utilizes corm-based vacuum infiltration, *I. japonica* presents distinct challenges due to its unique rhizome structure, necessitating the development of customized methodologies. Therefore, establishing an efficient and effective research system for validating gene functions in *I. japonica* is crucial for advancing its genetic breeding studies. VIGS technology, with its advantages of not requiring genetic transformation, being independent of varieties, and being simple and efficient, is particularly suitable for gene function validation studies in monocotyledons like *I. japonica*. The TRV vector is currently the most widely used VIGS vector, known for its mild symptoms upon infection and high silencing efficiency across multiple plant species[32]. Therefore, TRV was selected as the expression vector in this study.

IjPDS identification and construction of the VIGS vector (pTRV2-*IjPDS*)

The first step in the VIGS experiment was to identify the target gene and analyze its sequence for conserved regions. The full-length *PDS* gene (*IjPDS*) was identified from the *I. japonica* transcriptome and verified by sequencing. The *IjPDS* gene is 1,399 bp long

and encodes a protein of 389 amino acids. To confirm the conservation of *IjPDS*, its sequence was compared with the *PDS* sequences of model plants and related monocot species, such as *A. thaliana*, wheat, daffodil, gladiolus, and musk lily. The alignment revealed a high sequence homology of 83.61% (Fig. 2a), suggesting that *IjPDS* is highly conserved.

Next, a VIGS vector targeting *IjPDS* was constructed based on this conserved sequence (Fig. 2b). The *IjPDS* gene fragment was amplified, and the resulting sequence was inserted into the pTRV2 plasmid, which was then digested with *Xba* I and *Sac* I restriction enzymes. The recombinant plasmid, pTRV2-*IjPDS*, was generated by ligating the *IjPDS* gene fragment into the pTRV2 vector and transformed into *E. coli* DH5α cells. Subsequently, the pTRV1 and pTRV2-*IjPDS* vectors were introduced into *A. tumefaciens* and the bacterial solution containing pTRV1 and pTRV2 was mixed in a ratio of 1:1 for infecting receptor plants (Fig. 2b).

Several visual reporter genes are commonly used in the VIGS system to monitor gene silencing in plants. These include genes involved in anthocyanin, chlorophyll, and carotenoid biosynthesis, such as *PDS*, *Chalcone Synthase* (*CHS*), *Filamentation Temperature-Sensitive H* (*Ftsh*), and *Magnesium-Chelatase H Subunit* (*ChlH*)[33–36]. The *PDS* gene, which encodes phytoene desaturase, plays a key role

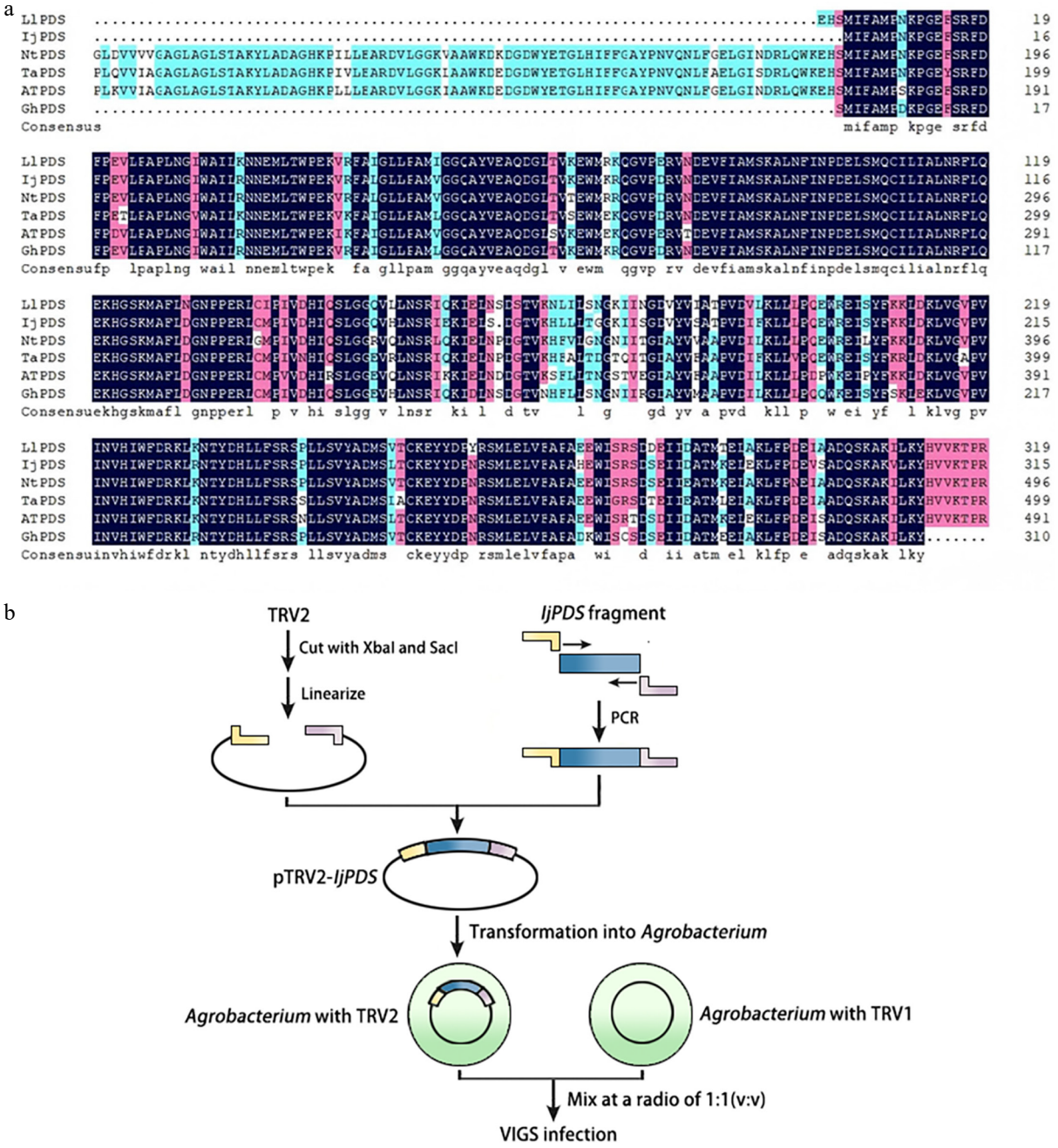

Fig. 2 Identification of *IjPDS* and construction of VIGS vector (pTRV2-*IjPDS*). (a) Multiple sequence alignment of the *PDS* gene from *Iris japonica*, a model plant, and related monocot species to identify conserved sequences. *LlPDS*: *Lilium longiflorum*, BAV93014.1; *IjPDS*: *Iris japonica*, T02.PB9671; *NtPDS*: *Narcissus tazetta*, AFH53816.1; *TaPDS*: *Triticum aestivum*, ACL36586.1; *AtPDS*: *Arabidopsis thaliana*, AT4G14210; *GhPDS*: *Gladiolus hybrid*, AGI17588.1. The red rectangles indicate the target fragment used for silencing *IjPDS*. (b) Procedure for pTRV2-*IjPDS* construction and agro-infiltration. The yellow and pink lines represent adaptors used in ligation-independent cloning, while the blue lines represent the target *IjPDS* fragment.

in carotenoid biosynthesis in photosynthetic tissues. Silencing of this gene leads to a bleached phenotype[37,38]. Therefore, *IjPDS* was selected as a visual marker to assess the efficiency of the TRV-based vector in this study.

In monocot species, the inoculation method plays a crucial role in achieving successful gene silencing. To silence a single gene within a gene family, the target sequence inserted into the viral vector should be derived from the 3' or 5' untranslated regions (UTR). For simultaneous silencing of multiple genes, the target sequence is typically selected from conserved gene regions[39,40].

Agrobacterium inoculation of *Iris japonica* receptor plants

To assess whether the TRV vector could effectively induce *IjPDS* gene silencing in *I. japonica*, *Agrobacterium* was transformed with pTRV1 and pTRV2-*IjPDS* vectors, which were then mixed in equal proportions. The inoculation of *I. japonica* was carried out through vacuum infiltration, a method known to enhance infection efficiency in the VIGS system.

For the inoculation procedure, rhizomes and leaves of *I. japonica* plants were subjected to infection. The leaves were trimmed to approximately 10 cm in length, and 2–3 punctures were made into the rhizomes or leaf base using toothpicks. Seedlings of different ages were immersed in the infection solution and subjected to vacuum infiltration. Subsequently, the treated plants, along with control plants that did not receive the bacterial solution, were placed in the dark for 3 d and then cultured for an additional 28 d to monitor phenotypic changes (Fig. 3a–c).

The treated *I. japonica* plants began to exhibit a silenced phenotype two weeks after inoculation, characterized by white spots or fan-like patterns on the newly developed green leaves due to the silencing of *IjPDS* (Fig. 3d). In contrast, the control group leaves remained green. These results confirm that *IjPDS* gene silencing was successfully induced in *Iris* and that the TRV-mediated VIGS system is effective for regulating genes in *I. japonica*.

Various leaf infiltration methods, including needle-less infiltration, vacuum infiltration, and high-pressure spraying, have been employed for different plant species and VIGS vectors. VIGS experiments typically utilized a range of plant organs, such as bulbs, leaves, cornels, roots, fruits as well as flowers[32]. In addition to living plants, *in vitro* organs—such as stem segments, cotyledon segments, and tepal discs—can also serve as inoculation acceptors[41]. For most herbs and younger seedlings, vacuum infiltration is a simple and effective method, whereas thicker, more rigid tissues tend to yield better results with needle syringe injections[42]. Unlike corm-based species such as *Gladiolus* or bulb-based species such as *Lilium*, *I. japonica* has a rhizomatous structure that is particularly sensitive to standard vacuum infiltration methods, often resulting in tissue necrosis and poor infection efficiency. To address these challenges, multiple parameters, including inoculation method, seedling age, and infiltration conditions, should be optimized to enable stable and efficient gene silencing with minimal tissue damage. For example, petal and inflorescence tissues were selected as acceptors for VIGS in *Agapanthus praecox* ssp. *orientalis*, where vacuum infiltration and a combined method of injection and soaking were employed[43]. The infection efficiency of the vacuum infiltration method was 66.67% while the injection method had an efficiency of only 26.47%, indicating that vacuum infiltration method provided a higher infection efficiency. Moreover, infiltration conditions, such as *Agrobacterium* concentration, play a crucial role in VIGS efficiency[44]. Specifically, an OD_{600} of 2.0 was found to provide the optimal conditions for tepal infiltration in VIGS experiments.

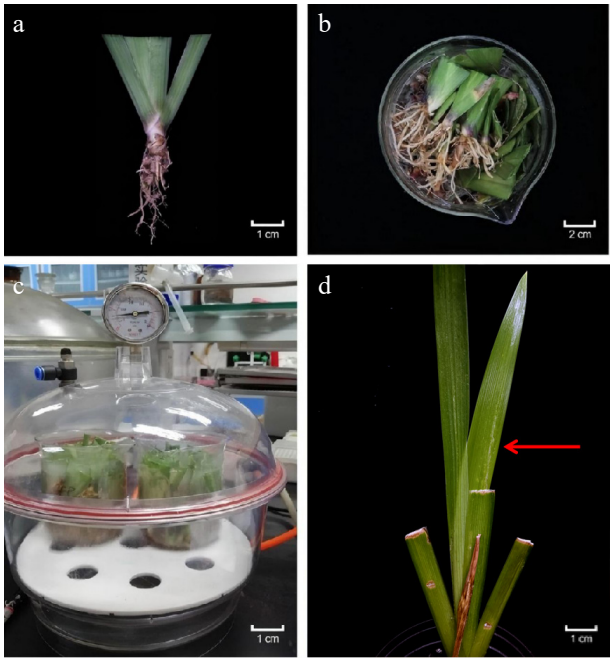

Fig. 3 *Agrobacterium tumefaciens* inoculation of *Iris japonica* receptor plants in the VIGS System. (a) Rhizomes and clipped leaves of receptor plants pricked with toothpicks. (b) Receptor plants placed in a beaker for inoculation with the prepared *A. inoculation* solution. (c) Receptor plants subjected to vacuum infiltration to enhance infection efficiency. (d) Photobleached phenotype observed in the newly developed leaves of silenced plant after two weeks.

Validation of pTRV2-GFP vector in the leaves of *Nicotiana tabacum*

To establish a visualizable VIGS system, the pTRV2 vector was modified by deleting the stop codon of the ORF of CP and tagging it with the Green Fluorescent Protein (GFP) ORF sequence via overlap PCR. The modified vector was named pTRV2-GFP. After transforming *Agrobacterium* with pTRV1 and pTRV2-GFP vectors and mixing the solutions, the pTRV2-GFP infection solution was injected into the tobacco (*Nicotiana tabacum*) leaves. The treated plants and wild-type plants were dark-cultured for 3 d and then exposed to bright (Fig. 4a, b) and ultraviolet light (Fig. 4c, d) for macro-level observation. GFP fluorescence was first detected in the injected areas at 6 d post-inoculation (dpi), confirming the successful viral spread and the feasibility of the VIGS system. At the micro level, GFP fluorescence was detected in mesophyll cells using laser confocal microscopy, further validating the functionality of the pTRV2-GFP expression system (Fig. 4e, f). These findings confirm that the pTRV2-GFP vector successfully facilitated GFP expression in tobacco, proving the efficacy of the VIGS system for functional gene studies in this model plant. The tobacco VIGS system lays a foundation for further applications of this system in gene silencing experiments of *Iris*.

The VIGS system has now been successfully established in various plant species and is widely used for identifying functional genes. VIGS technology was first applied to tobacco[45] and has since been extensively utilized for gene function analysis, especially in plants that are challenging to genetically transform. Tobacco, as a common host for VIGS studies, has been instrumental in investigating a wide range of genes, including those related to disease resistance and development. This highlights the utility of VIGS in the rapid identification of gene function[46]. Among the different infiltration methods, leaf infiltration remains one of the most frequently used techniques, particularly in tobacco[47].

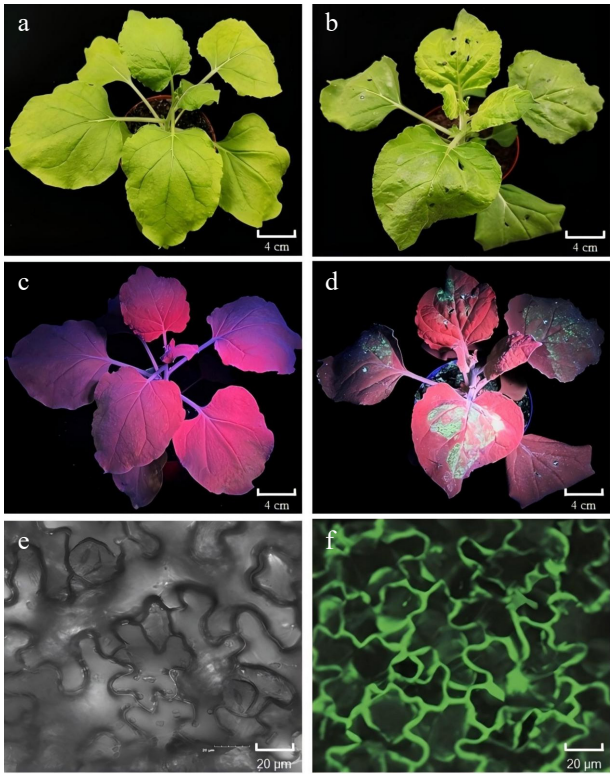

Fig. 4 Validation of the pTRV2-GFP vector in tobacco (*Nicotiana tabacum*) leaves. (a), (b) Photographs of tobacco leaves taken 6 d post-infiltration (dpi) without or with pTRV2-GFP, captured under open-field lighting conditions. (c), (d) GFP expression observed under ultraviolet (UV) light in tobacco leaves at 6 dpi, without and with pTRV2-GFP. GFP fluorescence was detected in regions corresponding to GFP expression in the treated areas. (e), (f) GFP fluorescence detected using a laser scanning confocal microscope (Olympus FV3000, Kyoto, Japan) in tobacco leaves at 6 dpi without or with pTRV2-GFP. Fluorescent regions indicate GFP expression in the treated leaves.

Application of pTRV2-GFP vector in *Iris japonica*

To further verify the feasibility of the VIGS system in *I. japonica*, the pTRV2-GFP vector was introduced into the leaves of young *I. japonica* plants. The effectiveness of the pTRV2-GFP vector in inducing GFP expression was assessed by observing fluorescence patterns and conducting RT-PCR analysis.

Following infiltration, 30 plants were evenly divided into three biological replicates in wild-type *I. japonica* (untreated), pTRV2-treated (pTRV2) and pTRV2-GFP-treated (pTRV2-GFP) groups respectively, and incubated in the dark for 3 d, followed by growth under standard conditions. A week later, the leaf morphology and fluorescence were examined under ultraviolet (UV) light, and GFP fluorescence in mesophyll cells was further analyzed using a laser scanning confocal microscope. Additionally, RT-PCR was performed to verify the presence of GFP expression and the successful inoculation of the TRV-based vectors.

Under UV light, strong fluorescence in the leaves of *I. japonica* plants treated with pTRV2-GFP was detected (Fig. 5a), indicating successful GFP expression. The fluorescence was widespread across the treated leaves, while untreated plants and pTRV2-treated plants exhibited no noticeable fluorescence. These results confirm the successful expression of GFP in the pTRV2-GFP-treated group. Confocal microscopy observations (Fig. 5b) further supported these findings, revealing distinct GFP fluorescence localized in the mesophyll cells of 6, 5, and 5 pTRV2-GFP-treated plants in each replicate. This results in an overall infection efficiency of 53.33 ± 5.77%, demonstrating effective gene expression at the cellular level. In contrast, GFP fluorescence was absent from both the wild-type and pTRV2-treated plants, providing additional evidence for the successful expression of GFP in the experimental group.

Finally, RT-PCR analysis (Fig. 5c) confirmed the presence of the TRV and GFP sequences in the pTRV2-GFP-treated group, with a prominent PCR band around 1,500 bp, corresponding to the expected size of the pTRV2-GFP construct. The pTRV2-treated group, treated with TRV alone, displayed a smaller band (~200 bp), consistent with the TRV vector amplification. No TRV transcripts were detected in wild-type plants, further validating the successful inoculation of the TRV-based vector and GFP expression in the treatment group.

When silencing genes that do not produce observable phenotypes, GFP is commonly used as a visual reporter to assess the efficiency of target gene silencing in various plants[48]. Unlike traditional TRV-VIGS workflows in tobacco[49], GFP co-silencing was introduced for real-time and visual monitoring of silencing efficiency. This approach eliminates reliance on molecular validation and enhances experimental throughput, particularly in species lacking stable transformation systems. The results from this study collectively demonstrate that the pTRV2-GFP vector successfully induced GFP expression in *I. japonica* leaves, thereby establishing the pTRV2-GFP-based VIGS system in this species. This work lays a foundation for developing a functional VIGS platform for gene silencing studies in *Iris* species.

Phenotypic and molecular validation of *IjPDS* silencing in *Iris japonica*

To verify the applicability of the TRV-VIGS system in silencing homologous genes of *Iris* species, the pTRV2-*IjPDS* expression vector was used to infect *I. japonica* and assess the silencing effect of the *IjPDS* gene. The *PDS* gene is involved in the biosynthesis of carotenoids, which has been reported in many plant species. It can serve as a visible marker to evaluate and monitor the silencing efficiency of VIGS, as its knockdown in plants can lead to an albino phenotype, due to the lack of chlorophyll[50]. After injecting infection solutions into *I. japonica*, 30 plants were evenly divided into three replicates in wild type (untreated), pTRV2-treated and pTRV2-*IjPDS*-treated groups respectively, and incubated in the dark for 3 d, followed by 28 d of the routine culture in a growth chamber. After four weeks, leaf phenotypes were observed and recorded under bright light, and the infection efficiency at different seedling ages was calculated. Meanwhile, one week post-infection, RT-PCR was performed on the leaves of all groups to verify successful infection with pTRV2 and pTRV2-*IjPDS* vectors based on the band size. qPCR was also carried out to evaluate the expression level of *IjPDS* at the molecular level.

Four weeks after infection, three, four, and four plants of *I. japonica* infected with the pTRV2-*IjPDS* vector in each replicate displayed a prominent phenotype, with a broad and distinct whitening effect, resulting in an overall silencing efficiency of 36.67 ± 5.77%. This consistent silencing phenotype indicates effective silencing of the *IjPDS* gene in *I. japonica*. In contrast, the leaves of untreated plants and pTRV2-infected plants remained green (Fig. 6a). These observations confirm the successful establishment of the TRV-mediated VIGS system in *I. japonica*, demonstrating that functional genes in *Iris* can be effectively silenced using this system. Besides, the gene silencing efficiency between the pTRV2-GFP vector and the unmodified pTRV2 vector was compared by inserting the same *IjPDS* gene fragment into both constructs (Table 2). The silencing efficiencies were 36.67% for pTRV2-*IjPDS* and 33.33% for pTRV2-GFP-*IjPDS*, which showed no significant difference in silencing efficiency between the two treatments. These findings suggest that the

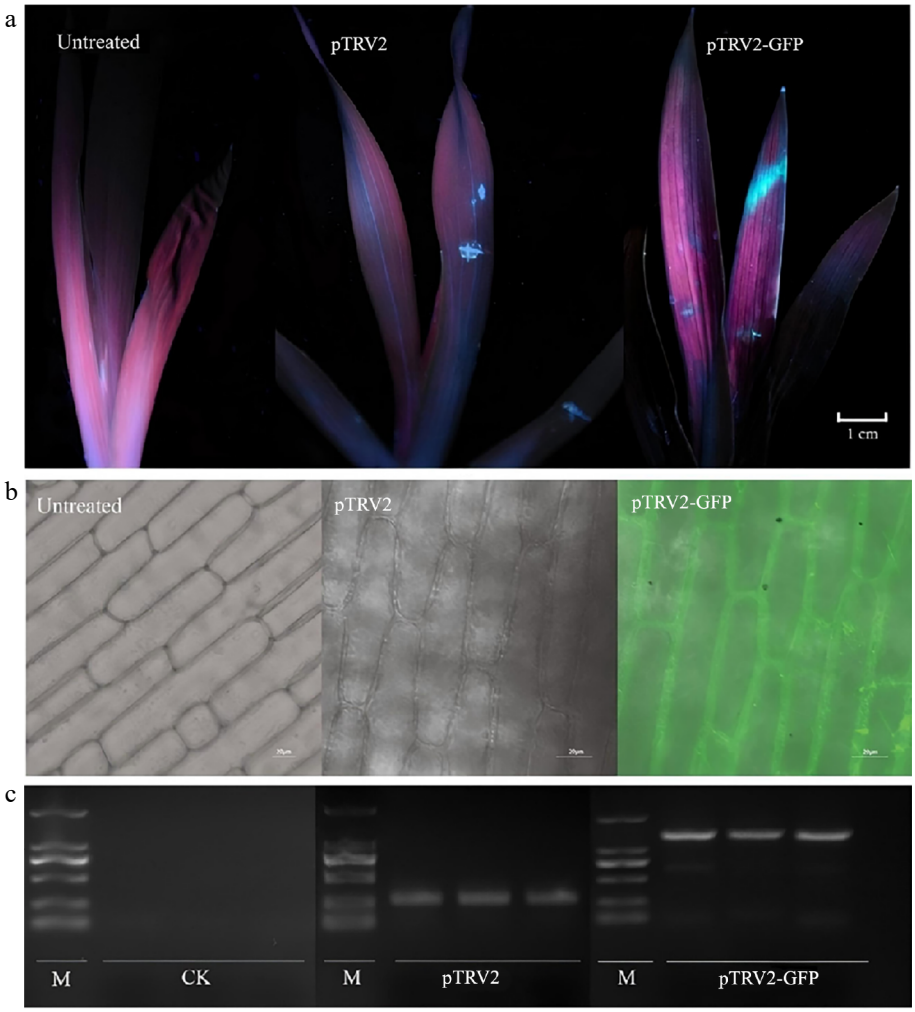

Fig. 5 Application of the pTRV2-GFP vector in *Iris japonica*. (a) GFP expression observed under ultraviolet (UV) light in *I. japonica* leaves 7 d post-infiltration (dpi), comparing untreated, pTRV2-treated, and pTRV2-GFP-treated leaves. UV fluorescence was detected in the regions on the leaves treated with pTRV2 and pTRV2-GFP, confirming GFP expression. (b) GFP expression observed under a laser scanning confocal microscope (Olympus FV3000, Kyoto, Japan) in *I. japonica* leaves at 7 dpi, comparing untreated, pTRV2-treated and pTRV2-GFP-treated leaves, confirming successful expression. GFP fluorescence was detected in the regions of the pTRV2-GFP-treated leaves, confirming successful expression. (c) PCR validation of GFP expression in *I. japonica* leaves 7 dpi, comparing untreated, pTRV2-treated, and pTRV2-GFP-treated leaves. A GFP-specific band was observed in the pTRV2-GFP-treated leaves, indicating the successful inoculation of pTRV2 and pTRV2-GFP vectors in *I. japonica*.

addition of the GFP cassette does not negatively impact silencing efficacy and provides an added advantage of non-destructive tracking.

RT-PCR analysis of the TRV vector fragment in the untreated, pTRV2-treated, and pTRV2-*IjPDS*-treated groups showed the successful insertion of the *IjPDS* gene fragment into the TRV vector (Fig. 6b). The larger band (~550 bp) observed in the pTRV2-*IjPDS*-treated plants corresponds to the TRV vector with the inserted *IjPDS* gene fragment (281 bp), while the smaller band (~250 bp) was corresponded to the empty TRV vector. No TRV vector fragment was detected in untreated plants, confirming the successful insertion and silencing of the *IjPDS* gene.

The downregulation of *IjPDS* expression was further validated by qPCR analysis in the pTRV2-*IjPDS*-treated plants (Fig. 6c). Compared to the untreated and TRV-treated groups, the gene expression level of *IjPDS* in the pTRV2-*IjPDS*-treated group was reduced by nearly 9-fold on average, providing strong molecular evidence for the successful silencing of the *IjPDS* gene. This significant decrease in gene expression further supports the efficacy of the TRV-VIGS system in silencing the *IjPDS* gene in *I. japonica*.

To identify the optimal seedling age for TRV-VIGS infection, 30 plants of each age group (one month, two months, one year, and two years) were evenly divided into three replicates and assessed for gene silencing efficiency. The results indicated that gene silencing efficiency was highest in one-year-old plants (36.67 ± 5.77%, with three, three, and four plants per replicate exhibiting photobleached phenotypes), followed by two-month-old plants (23.33 ± 5.77%, with two, two, and three plants per replicate), two-year-old plants (13.33 ± 5.77%, with two, one, and one plants per replicate), and one-month-old plants (10.00%, with two, one, and zero plants per replicate) (Fig. 6d). These findings suggest that gene silencing efficiency improves with seedling age up to one year, but decreases beyond that age. These results suggested that although the silencing of *PDS* can lead to visible photobleaching, it can also result in wilting and plant death. Therefore, it cannot be used for gene silencing throughout the entire plant growth period[51].

The plant material affected the efficiency of TRV-mediated VIGS. A semi-quantitative RT-PCR was performed in tomato to confirm *PDS* silencing[47]. In pTRV2-*IjPDS*-infected plants, the *PDS* expression was reduced by more than 78% compared with the TRV-infected

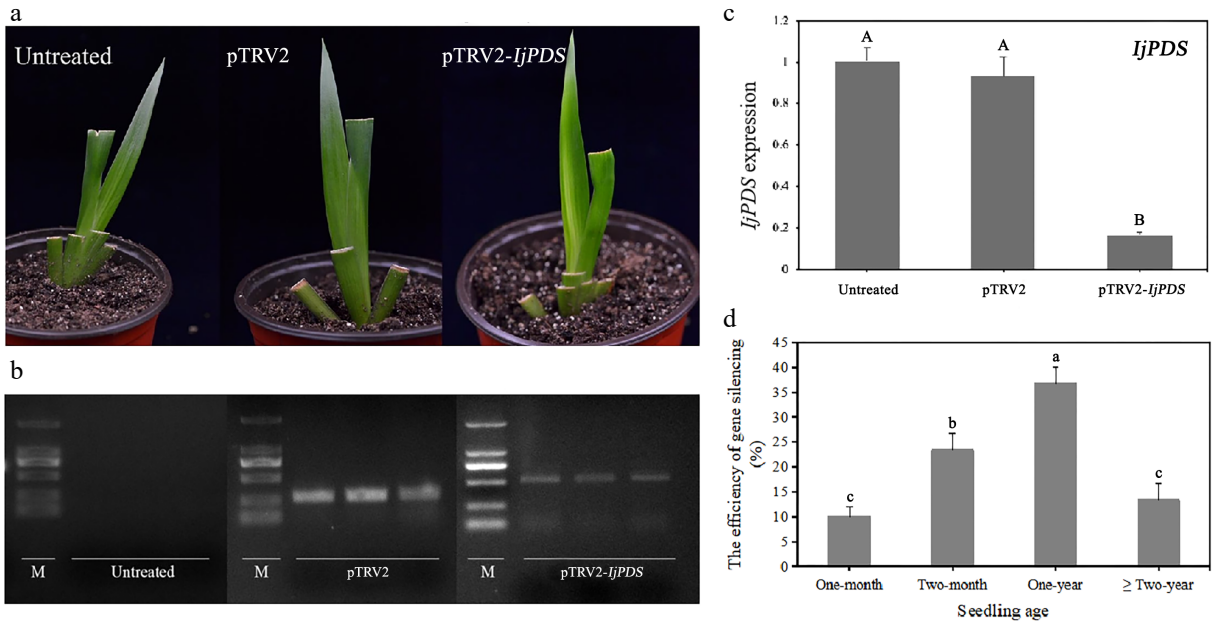

Fig. 6 Phenotype and molecular validation of *IjPDS* silencing in *Iris japonica*. (a) Phenotypic observations of untreated, pTRV2-treated, and pTRV2-*IjPDS*-treated *I. japonica* leaves at 28 d post-infiltration (dpi). A characteristic photobleached phenotype was observed in the newly developed leaves of pTRV2-*IjPDS*-treated plants at 28 dpi, indicating successful silencing of *IjPDS*. (b) RT-PCR analysis of *PDS* expression in *I. japonica* leaves at 28 dpi from untreated, pTRV2-treated, and pTRV2-*IjPDS*-treated plants. A larger specific band was observed in the pTRV2-*IjPDS*-treated leaves compared to the pTRV2-treated leaves, confirming the infection of the pTRV2-*IjPDS* vector. In contrast, there is no TRV band detected in untreated plants. (c) Quantitative real-time PCR (qPCR) analysis of *PDS* expression in *I. japonica* leaves at 28 dpi from untreated, pTRV2-treated, and pTRV2-*IjPDS*-treated plants. Reduced *PDS* expression was detected in the pTRV2-*IjPDS*-treated plants, confirming successful silencing of *IjPDS* in *I. japonica* leaves. (d) Comparison of infection efficiency at different seedling ages, demonstrating the optimal age for successful silencing in *I. japonica*. Each age group consists of three sets of uniformly growing plants, with ten plants per set. The data represent the mean values ± standard error. Different letters in (c) and (d) indicate significant differences at $p < 0.05$, following statistical analysis by ANOVA.

Table 2. Efficiency assessment of TRV-VIGS system using pTRV2-GFP and pTRV2-*IjPDS* visual vectors.

Efficiency	Vector		
Group	pTRV2-GFP	pTRV2-*IjPDS*	pTRV2-GFP-*IjPDS*
1	60%	30%	30%
2	50%	40%	30%
3	50%	40%	40%
Average	53.33%	36.67%	33.33%
SD	5.77%	5.77%	5.77%
Significant differences indicated by different letters	a	b	b

controls. Besides, as a phenotypic scorable endogenous gene, *PDS* have also been tested as a positive controls in TRV-based VIGS in cotton, whose silencing showed the photobleaching effect[51]. The fact that TRV effectively caused the VIGS of *PDS* in tomato also suggests that *PDS* could be used as a positive control in the VIGS system, and other nuclear genes could be targeted for silencing in a similar manner.

Construction of the TRV-VIGS system and its application in *Iris japonica*

Following the successful establishment of the TRV-mediated VIGS system in *I. japonica*, its application in related research was explored. Transcriptomic and genomic analyses were performed to predict key genes involved in specific biological processes (Fig. 7a). Using gene phylogenetic analysis, conserved domain sequence comparison, and bioinformatics tools, target genes were identified and their full-length sequences determined. The TRV-VIGS system was then employed for transient gene function verification, with target gene fragments inserted into the TRV vector and introduced into *Iris* via *Agrobacterium*-mediated methods (Fig. 7b). The viral spread and replication induced gene silencing, leading to the inhibition of target gene expression. By comparing phenotypic, physiological, and biochemical differences between gene-silenced plants and controls, as well as analyzing the predicted downstream gene expression, the function of the target genes were confirmed and their regulatory mechanisms elucidated (Fig. 7c). This approach also enabled the investigation of gene regulatory relationships and the construction of a gene regulation network.

Beyond gene function verification, VIGS technology has a broad range of applications in plant research to investigate metabolic pathways, disease resistance, and traits related to growth and development[43]. In evolutionary and developmental biology, it can be used to explore the functional conservation and differentiation of homologous genes across plant species. By comparing phenotypic differences after silencing specific genes, VIGS offers valuable insights into the evolution of gene functions[52]. In secondary metabolism, silencing key enzyme genes involved in the metabolic pathway enables the analysis of changes in metabolites, biosynthetic pathway, and their regulatory mechanism. In plant-pathogen interactions, VIGS can be applied to silence plant immune-related genes, revealing changes in plant resistance and identifying critical nodes in immune signaling pathways. Additionally, VIGS has been used to study the molecular pathways involved in root nodule formation and the exchange of substrates between host plants and rhizobia[37].

However, VIGS protocols are not universally transferable, even within the Iridaceae family. For instance, *Gladiolus* and *Iris* differ in

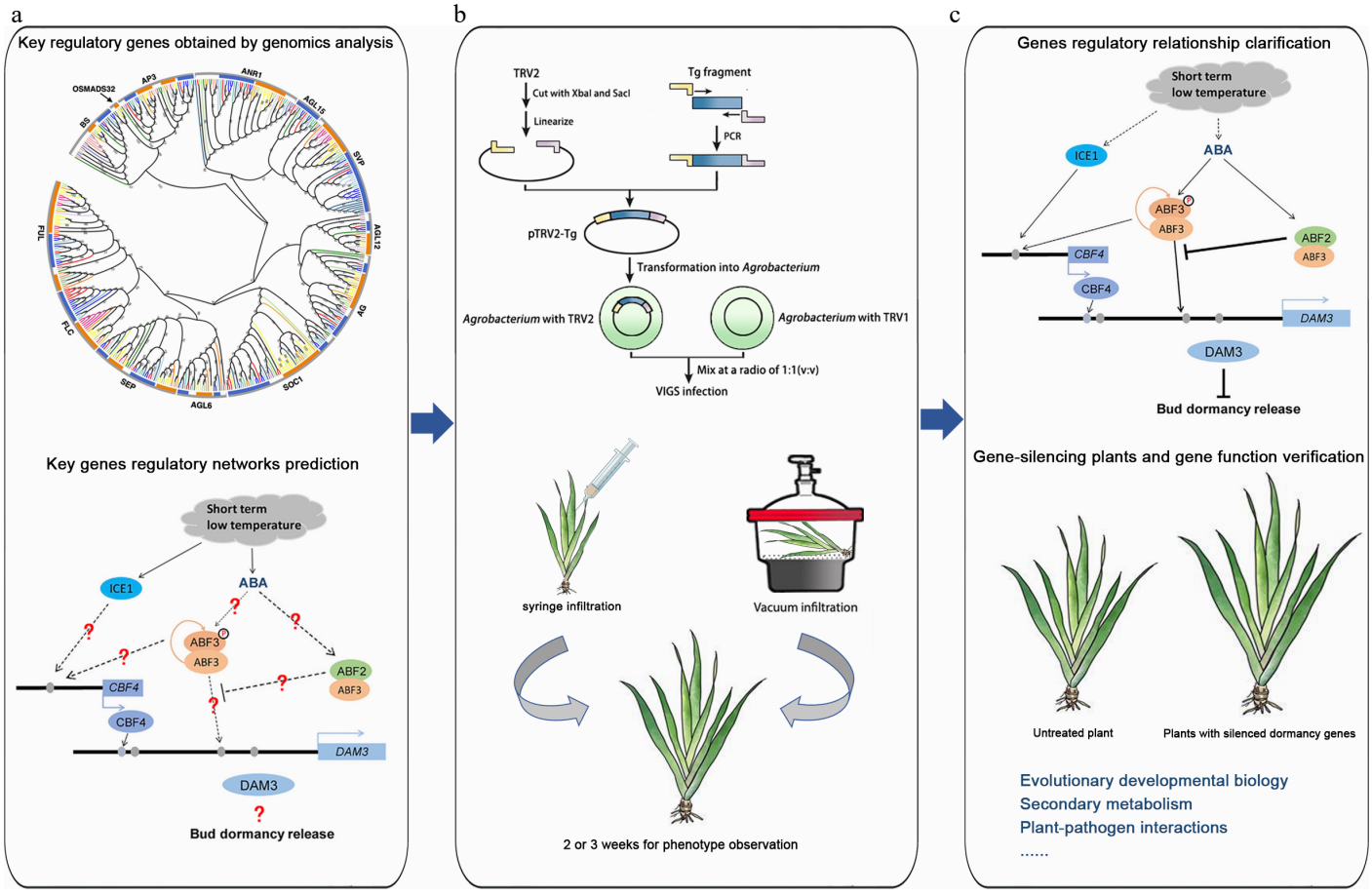

Fig. 7 The application of the TRV-VIGS system in plant research using *Iris japonica* as an example. (a) Genomics analysis. Key regulatory genes were identified through genomics analysis, and the regulatory networks of these genes were predicted. The graphs of phylogenetic analysis and regulatory network were modified from Li et al.[5] and Yang et al.[57], respectively. (b) Homologous gene verification of homologous gene function by VIGS. A target gene fragment was constructed into the TRV vector, and various *Agrobacteria*-mediated methods, such as syringe infiltration and vacuum infiltration, were used to infect *Iris* leaves to verify homologous gene function. (c) Gene function research. The regulatory relationships between genes were explored, gene-silenced plants were obtained, and gene functions were validated. Additionally, VIGS technology is not limited to gene function verification but can also be applied to research in evolutionary and developmental biology, secondary metabolism, immune interactions, and symbiotic relationships.

secondary metabolism[53] and stress-response pathways, necessitating species-specific optimization. This study provides a foundation for adapting VIGS to diverse monocot lineages.

Building on the initial success of the TRV-VIGS system in *I. japonica*, future studies will aim to improve silencing efficiency by evaluating additional factors, such as *Agrobacterium* strains, infection concentrations, and infection methods. For example, commonly used strains (e.g., GV3101, EHA105, LBA4404) will be compared across a range of bacterial densities (OD_{600} values), and alternative infection techniques, such as rub-inoculation and spray-inoculation, will be explored. These efforts will contribute to the development of a more efficient and standardized VIGS system for *I. japonica*.

In summary, the TRV-mediated VIGS system developed in this study provides a powerful tool for in-depth understanding of gene function and biological processes in *Iris*, whose stable genetic transformation protocols were hard to establish. Compared to traditional stable transformation methods, VIGS offers rapid gene function analysis by silencing target genes in the current generation of infected plants, avoiding the need for genetic transformation, and providing high-throughput screening capabilities[54]. Although VIGS usually induces transient gene silencing in various plants, there is some evidence that the gene silencing effect can be transmitted to progeny[55,56]. To sum up, VIGS is more straightforward, efficient, and time-saving than traditional stable transformation methods. Its expanding application has advanced plant science, and will also promote the development of *Iris* research to a certain extent in the future, making it an essential technology in the field.

Author contributions

The authors confirm contributions to the paper as follows: study conception and design: Luo C, Xia Y, Li D; data collection: Luo C, Wu Z, Zhang J; analysis and interpretation of results: Luo C, Shao L; draft manuscript preparation: Luo C, Wu Z, Li D. All authors reviewed the results and approved the final version of the manuscript.

Data availability

All data generated or analyzed during this study are included in this published article.

Acknowledgments

This work was supported by the general project of the Zhejiang Provincial Department of Education (Grant No. Y202456763), the Zhejiang Sci-Tech University Start-up Fund (Grant No. 24052162-Y), the China Postdoctoral Science Foundation (Grant No. 2021M692790), and the National Natural Science Foundation of China (NSFC) (Grant No. 31901352).

Conflict of interest

The authors declare that they have no conflict of interest.

Dates

Received 20 March 2025; Revised 16 June 2025; Accepted 15 July 2025; Published online 16 September 2025

References

1. Singab ANB, Ayoub IM, El-Shazly M, Korinek M, Wu TY, et al. 2016. Shedding the light on Iridaceae: ethnobotany, phytochemistry and biological activity. *Industrial Crops and Products* 92:308−35
2. Luan ZJ, Li PP, Li D, Meng XP, Sun J. 2020. Optimization of supercritical-CO_2 extraction of Iris *lactea* seed oil: component analysis and antioxidant activity of the oil. *Industrial Crops and Products* 152:112553
3. Fan Z, Gao Y, Ren Y, Guan C, Liu R, et al. 2020. To bloom once or more times: the reblooming mechanisms of Iris germanica revealed by transcriptome profiling. *BMC Genomics* 21:553
4. Li D, Zhang J, Zhang J, Li K, Xia Y. 2017. Green period characteristics and foliar cold tolerance in 12 Iris species and cultivars in the Yangtze Delta, China. *HortTechnology* 27(3):399−407
5. Li D, Shao L, Zhang J, Wang X, Zhang D, et al. 2022. MADS-box transcription factors determine the duration of temporary winter dormancy in closely related evergreen and deciduous Iris spp. *Journal of Experimental Botany* 73(5):1429−49
6. Xu T, Zhang J, Shao L, Wang X, Zhang R, et al. 2022. Later growth cessation and increased freezing tolerance potentially result in later dormancy in evergreen iris compared with deciduous iris. *International Journal of Molecular Sciences* 23(19):11123
7. Jozghasemi S, Rabiei V, Soleymani A, Khalighi A. 2015. Evaluation of the pigments concentration in the Iris species native to Iran. *Journal of Biodiversity and Environmental Sciences* 6(1):557−61
8. Zhang X, Yang H, Wu B, Chen H. 2022. The chloroplast genome of the *Iris japonica* Thunberg (Butterfly flower) reveals the genomic and evolutionary characteristics of *Iris* species. *Mitochondrial DNA Part B* 7(10):1776−82
9. Shi GR, Wang X, Liu YF, Zhang CL, Ni G, et al. 2016. Novel iridal metabolites with hepatoprotective activities from the whole plants of *Iris japonica*. *Tetrahedron Letters* 57(51):5761−63
10. Shi GR, Wang X, Liu YF, Zhang CL, Ni G, et al. 2017. Bioactive flavonoid glycosides from whole plants of *Iris japonica*. *Phytochemistry Letters* 19:141−44
11. Pan ZJ, Chen YY, Du JS, Chen YY, Chung MC, et al. 2014. Flower development of *Phalaenopsis* orchid involves functionally divergent *SEPALLATA*-like genes. *New Phytologist* 202:1024−42
12. Hsu HF, Hsu WH, Lee YI, Mao WT, Yang JY, et al. 2015. Model for perianth formation in orchids. *Nature Plants* 1:15046
13. Jang S, Choi SC, Li HY, An G, Schmelzer E. 2015. Functional characterization of *Phalaenopsis aphrodite* flowering genes *PaFT1* and *PaFD*. *PLoS One* 10:e0134987
14. Min D, Zhang X, Ji N, Li F, Shao S. 2017. The application of TRV-mediated VIGS technique in the study of gene function in fruits and vegetables. *Plant Physiology Journal* 53:159−66
15. Yang W, Chen X, Chen J, Zheng P, Liu S, et al. 2023. Virusinduced gene silencing in the tea plant (*Camellia sinensis*). *Plants* 12:3162
16. Zulfiqar S, Farooq MA, Zhao T, Wang P, Tabusam J, et al. 2023. Virus-induced gene silencing (VIGS): a powerful tool for crop improvement and its advancement towards epigenetics. *International Journal of Molecular Sciences* 24:5608
17. Yang X, Liu Z, Li Y, Zou J, Zheng Y, et al. 2024. Construction and optimization of the TRV-mediated VIGS system in *Areca catechu* embryoids. *Scientia Horticulturae* 338:113621
18. Kant R, Dasgupta I. 2019. Gene silencing approaches through virus-based vectors: speeding up functional genomics in monocots. *Plant Molecular Biology* 100:3−18
19. Ratcliff F, Martin-Hernandez AM, Baulcombe DC. 2001. Technical advance: tobacco rattle virus as a vector for analysis of gene function by silencing. *The Plant Journal* 25:237−45
20. Tiedge K, Destremps J, Solano-Sanchez J, Arce-Rodriguez ML, Zerbe P. 2022. Foxtail mosaic virus-induced gene silencing (VIGS) in switchgrass (*Panicum virgatum* L.). *Plant Methods* 18:71
21. Tuo D, Zhou P, Yan P, Cui H, Liu Y, et al. 2021. A cassava common mosaic virus vector for virus-induced gene silencing in cassava. *Plant Methods* 17:74
22. Zhang J, Yu D, Zhang Y, Liu K, Xu K, et al. 2017. Vacuum and co-cultivation agroinfiltration of (germinated) seeds results in tobacco rattle virus (*TRV*) mediated whole-plant virus-induced gene silencing (VIGS) in wheat and maize. *Frontiers in Plant Science* 8:393
23. Zhou P, Peng J, Zeng M, Wu L, Fan Y, et al. 2021. Virus-induced gene silencing (VIGS) in Chinese narcissus and its use in functional analysis of *NtMYB3*. *Horticultural Plant Journal* 7(6):565−72
24. Deng X, Bashandy H, Ainasoja M, Kontturi J, Pietiäinen M, et al. 2014. Functional diversification of duplicated chalcone synthase genes in anthocyanin biosynthesis of *Gerbera hybrida*. *New Phytologist* 201(4):1469−83
25. Jing W, Gong F, Liu G, Deng Y, Liu J, et al. 2023. Petal size is controlled by the MYB73/TPL/HDA19-miR159-CKX6 module regulating cytokinin catabolism in *Rosa hybrida*. *Nature Communications* 14(1):7106
26. Lu J, Zhang G, Ma C, Li Y, Jiang C, et al. 2024. The F-box protein RhSAF destabilizes the gibberellic acid receptor RhGID1 to mediate ethylene-induced petal senescence in rose. *The Plant Cell* 36(5):1736−54
27. Liang Y, Gao Q, Li F, Du Y, Wu J, et al. 2025. The giant genome of lily provides insights into the hybridization of cultivated lilies. *Nature Communications* 16(1):45
28. Pan W, Li J, Du Y, Zhao Y, Xin Y, et al. 2023. Epigenetic silencing of callose synthase by VIL1 promotes bud-growth transition in lily bulbs. *Nature Plants* 9(9):1451−67
29. Bruun-Rasmussen M, Madsen CT, Jessing S, Albrechtsen M. 2007. Stability of Barley stripe mosaic virus-induced gene silencing in barley. *Molecular Plant-Microbe Interactions* 20(11):1323−31
30. Ding XS, Mannas SW, Bishop BA, Rao X, Lecoultre M, et al. 2018. An improved brome mosaic virus silencing vector: greater insert stability and more extensive VIGS. *Plant Physiology* 176(1):496−510
31. Zhong X, Yuan X, Wu Z, Khan MA, Chen J, et al. 2014. Virus-induced gene silencing for comparative functional studies in *Gladiolus hybridus*. *Plant Cell Reports* 33:301−31
32. He G, Zhao X, Xu Y, Wang Y, Zhang Z, et al. 2023. An efficient virus-induced gene silencing (VIGS) system for gene functional studies in *Miscanthus*. *GCB Bioenergy* 15:805−20
33. Chen JC, Jiang CZ, Gookin T, Hunter D, Clark D, et al. 2004. Chalcone synthase as reporter in virus-induced gene silencing studies of flower senescence. *Plant Molecular Biology* 55:521−30
34. Saitoh H, Terauchi R. 2002. Virus-induced silencing of *FtsH* gene in *Nicotiana benthmiana* causes a striking bleached leaf phenotype. *Genes & Genetic Systems* 77:335−40
35. Yuan C, Li C, Yan L, Jackson AO, Liu Z, et al. 2011. A high throughput barley stripe mosaic virus vector for virus induced gene silencing in monocots and dicots. *PLoS One* 6:e26468
36. Mancinotti D, Rodriguez MC, Frick KM, Dueholm B, Jepsen DG, et al. 2021. Development and application of a virus-induced gene silencing protocol for the study of gene function in narrow-leafed lupin. *Plant Methods* 17:131
37. Dommes AB, Gross T, Herbert DB, Kivivirta KI, Becker A. 2019. Virus-induced gene silencing: empowering genetics in non-model organisms. *Journal of Experimental Botany* 70:757−70
38. Nisar N, Li L, Lu S, Khin NC, Pogson BJ. 2015. Carotenoid metabolism in plants. *Molecular Plant* 8:68−82
39. Stratmann JW, Hind SR. 2011. Gene silencing goes viral and uncovers the private life of plants. *Entomologia Experimentalis et Applicata* 140:91−102
40. Lee WS, Rudd JJ, Kanyuka K. 2015. Virus induced gene silencing (VIGS) for functional analysis of wheat genes involved in *Zymoseptoria tritici* susceptibility and resistance. *Fungal Genetics and Biology* 79:84−88
41. He G, Zhang R, Jiang S, Wang H, Ming F. 2023. The MYB transcription factor *RcMYB1* plays a central role in rose anthocyanin biosynthesis. *Horticulture Research* 10(6):uhad080

42. Dalakouras A, Jarausch W, Buchholz G, Bassler A, Braun M, et al. 2018. Delivery of hairpin RNAs and small RNAs into woody and herbaceous plants by trunk injection and petiole absorption. *Frontiers in Plant Science* 9:1253
43. Chen G, Song J, Zhang Y, Guo X, Shen X. 2024. Development and application of virus-induced gene silencing (VIGS) for studying *ApTT8* gene function in *Agapanthus praecox* ssp. *orientalis*. *Scientia Horticulturae* 324:112595
44. Li G, Li Y, Yao X, Lu L. 2023. Establishment of a virus-induced gene-silencing (VIGS) system in tea plant and its use in the functional analysis of *CsTCS1*. *International Journal of Molecular Sciences* 24:392
45. Kumagai MH, Donson J, Della-Cioppa G, Harvey D, Hanley K, et al. 1995. Cytoplasmic inhibition of carotenoid biosynthesis with virus-derived RNA. *Proceedings of the National Academy of Sciences of the United States of America* 92:1679–83
46. Liu M, Liu L, Wu H, Gu Q. 2018. Research progress in VIGS technology and its application in Cucurbitaceae crops. *Journal of Fruit Science* 35:1422–29
47. Liu Y, Schiff M, Dinesh-Kumar SP. 2002. Virus-induced gene silencing in tomato. *The Plant Journal* 31:777–86
48. Singh B, Kukreja S, Salaria N, Thakur K, Gautam S, et al. 2019. VIGS: a flexible tool for the study of functional genomics of plants under abiotic stresses. *Journal of Crop Improvement* 33(5):567–604
49. Senthil-Kumar M, Mysore KS. 2014. Tobacco rattle virus–based virus-induced gene silencing in *Nicotiana benthamiana*. *Nature Protocols* 9:1549–62
50. Qi X, Mo Q, Li J, Zi Z, Xu M, et al. 2023. Establishment of virus-induced gene silencing (VIGS) system in *Luffa acutangula* using phytoene desaturase (*PDS*) and tendril synthesis related gene (*TEN*). *Plant Methods* 19:94
51. Tian Y, Fang Y, Zhang K, Zhai Z, Yang Y, et al. 2024. Applications of virus-induced gene silencing in cotton. *Plants* 13(2):272
52. Gomariz-Fernández A, Sánchez-Gerschon V, Fourquin C, Ferrándiz C. 2017. The role of *SHI*/*STY*/*SRS* genes in organ growth and carpel development is conserved in the distant eudicot species *Arabidopsis thaliana* and *Nicotiana benthamiana*. *Frontiers in Plant Science* 8:814
53. Abe F, Chen RF, Yamauchi T. 1991. Iridals from *Belamcanda chinensis* and *Iris japonica*. *Phytochemistry* 30(10):3379–82
54. Guo Q, Wang Y, Zou J, Jing H, Li D. 2023. Efficient isolation and transformation of protoplasts in coconut endosperm and leaves for gene function studies. *Tropical Plants* 2:16
55. Marton I, Zuker A, Shklarman E, Zeevi V, Tovkach A, et al. 2010. Nontransgenic genome modification in plant cells. *Plant Physiology* 154:1079–87
56. Senthil-Kumar M, Mysore KS. 2011. Virus-induced gene silencing can persist for more than 2 years and also be transmitted to progeny seedlings in *Nicotiana benthamiana* and tomato. *Plant Biotechnology Journal* 9:797–806
57. Yang Q, Yang B, Li J, Wang Y, Tao R, et al. 2020. ABA-responsive ABRE-BINDING FACTOR3 activates DAM3 expression to promote bud dormancy in Asian pear. *Plant, Cell & Environment* 43(6):1360–75